

## Temperature dependence of the kinetic isotope effect in $\beta$ -pinene ozonolysis

Iulia Gensch,<sup>1</sup> Werner Laumer,<sup>1</sup> Olaf Stein,<sup>1</sup> Beatrix Kammer,<sup>1</sup> Thorsten Hohaus,<sup>1,2</sup> Harald Saathoff,<sup>3</sup> Robert Wegener,<sup>1</sup> Andreas Wahner,<sup>1</sup> and Astrid Kiendler-Scharr<sup>1</sup>

Received 7 April 2011; revised 22 July 2011; accepted 23 July 2011; published 18 October 2011.

[1] The temperature dependence of the kinetic isotope effect (KIE) of  $\beta$ -pinene ozonolysis was investigated experimentally at 258, 273 and 303 K in the AIDA atmospheric simulation chamber. Compound specific carbon isotopic analysis of gas phase samples was performed off-line with a Thermo Desorption-Gas Chromatography-Isotope Ratio Mass Spectrometry (TD-GC-IRMS) system. From the temporal behavior of the  $\delta^{13}\text{C}$  of  $\beta$ -pinene a KIE of  $1.00358 \pm 0.00013$  was derived at 303 K, in agreement with literature data. Furthermore, KIE values of  $1.00380 \pm 0.00014$  at 273 K and  $1.00539 \pm 0.00012$  at 258 K were determined, showing an increasing KIE with decreasing temperature. A parameterization of the observed KIE temperature dependence was deduced and used in a sensitivity study carried out with the global chemistry transport model MOZART-3. Two scenarios were compared, the first neglecting, the second implementing the KIE temperature dependence in the simulations.  $\beta$ -Pinene stable carbon isotope ratio and concentration were computed, with emphasis on boreal zones. For early spring it is shown that when neglecting the temperature dependence of KIE, the calculated average age of  $\beta$ -pinene in the atmosphere can be up to two times over- or underestimated. The evolution of the isotopic composition of the major  $\beta$ -pinene oxidation product, nopinone, was examined using Master Chemical Mechanism (MCM) simulations. The tested hypothesis that formation of nopinone and its associated KIE are the determining factors for the observed  $\delta^{13}\text{C}$  values of nopinone is supported at high  $\beta$ -pinene conversion levels.

**Citation:** Gensch, I., W. Laumer, O. Stein, B. Kammer, T. Hohaus, H. Saathoff, R. Wegener, A. Wahner, and A. Kiendler-Scharr (2011), Temperature dependence of the kinetic isotope effect in  $\beta$ -pinene ozonolysis, *J. Geophys. Res.*, 116, D20301, doi:10.1029/2011JD016084.

### 1. Introduction

[2] The gas phase oxidative chemistry of volatile organic compounds (VOCs) contributes to tropospheric ozone production and secondary organic aerosol (SOA) formation, thus affecting human health and influencing the climate. A better understanding of VOC sources and processes is therefore needed for improved model predictions of future air quality and climate. This concerns in particular biogenic VOC (BVOC), whose emissions are globally estimated to be one order of magnitude higher than the anthropogenic VOC emissions [Guenther *et al.*, 1995; Guenther, 1999; Müller, 1992; Piccot *et al.*, 1992].

[3] Analysis and interpretation of stable isotope ratios is a useful tool in identifying and quantifying the sources of

VOCs, as well as their physical and chemical processing in the atmosphere [Rudolph and Czuba, 2000; Rudolph, 2007]. In addition to concentration measurements of reactive gases and information gained from transport models or meteorology, knowledge of the isotopic composition reduces uncertainties in describing the origin and evolution of studied air masses.

[4] The stable isotope ratio of a sample is reported using *delta* notation,  $\delta^{13}\text{C}$ , describing the per mil (‰) deviation from a standard:

$$\begin{aligned}\delta^{13}\text{C} &= \left( \frac{[^{13}\text{C}]_{\text{sample}}/[^{12}\text{C}]_{\text{sample}}}{[^{13}\text{C}]_{\text{std}}/[^{12}\text{C}]_{\text{std}}} - 1 \right) 1000\text{‰} \\ &= \left( \frac{^{13}R_{\text{sample}}}{^{13}R_{\text{std}}} - 1 \right) 1000\text{‰}\end{aligned}\quad (1)$$

where  $^{13}R_{\text{sample}} = [^{13}\text{C}]_{\text{sample}}/[^{12}\text{C}]_{\text{sample}}$  and  $^{13}R_{\text{std}} = [^{13}\text{C}]_{\text{std}}/[^{12}\text{C}]_{\text{std}}$  are the isotope ratios for the sample and for the working standard, respectively. In the present work, final  $\delta^{13}\text{C}$  values are reported relative to the international reference Vienna Pee Dee Belemnite (VPDB) [International Union of Pure and Applied Chemistry (IUPAC), 1994].

<sup>1</sup>Institut für Energie- und Klimaforschung, Troposphäre (IEK-8), Forschungszentrum Jülich GmbH, Jülich, Germany.

<sup>2</sup>Now at Aerodyne Research, Inc., Billerica, Massachusetts, USA.

<sup>3</sup>Institute for Meteorology and Climate Research (IMK-AAF), Karlsruhe Institute of Technology, Karlsruhe, Germany.

[5] Oxidation as the major VOC degradation reaction in the atmosphere generally results in fractionation between the light and heavy isotopes. This is caused by the change in the oxidation reaction rate ( $k$ ) when, instead of the pure  $^{12}\text{C}$  reactant, its  $^{13}\text{C}$  containing isotopologue is involved in the reaction. The kinetic isotope effect (KIE) describes this variation and is defined by

$$\text{KIE} = \frac{{}^{12}k}{{}^{13}k} \quad (2)$$

where  ${}^{12}k$  is the reaction rate of the pure  $^{12}\text{C}$  reactant and  ${}^{13}k$  is the reaction rate of the  $^{13}\text{C}$  containing isotopologue.

[6] Since the isotope fractionation effects are generally very small, the KIEs are converted, similar to delta values for stable isotope ratios, to per mil epsilon values, describing the relative difference of the reaction rate constants:

$$\epsilon = \frac{{}^{12}k - {}^{13}k}{{}^{13}k} 1000\text{‰} = (\text{KIE} - 1) 1000\text{‰} \quad (3)$$

Due to the kinetic isotope effect, the light isotopes accumulate in the products, while the reactants become enriched in heavy isotopes [Wang and Kawamura, 2006]. Rudolph and coworkers developed a laboratory method to determine the KIE of oxidation reactions relevant for the atmosphere, basing on compound specific stable isotope analyses [Anderson et al., 2003; Iannone et al., 2003; Fisseha et al., 2009].

[7] The kinetic isotope effect of a reaction can be determined in laboratory studies from measurements of concentration and  $\delta^{13}\text{C}$  of a VOC as function of reaction time. Explicitly, the KIE value is deduced from the experimental data as a function of concentrations and isotope ratios at time  $t$  and  $t = 0$  [Anderson et al., 2003] as follows:

$$\ln \left[ \frac{{}^{12}C_t}{{}^{12}C_0} \right] = \frac{\text{KIE}}{1 - \text{KIE}} \ln \left[ \frac{(\delta^{13}C_t + 1000)}{(\delta^{13}C_0 + 1000)} \right] \quad (4)$$

where  ${}^{12}C_t$  and  ${}^{12}C_0$  denote the concentration at time  $t$  and  $t = 0$ . In most of these studies, KIE was determined at room temperature or higher [Anderson et al., 2004a, 2004b; Anderson, 2005].

[8] For atmospheric samples, the KIE value can be used to determine the average time passed since emission of a single species ( $t_{\text{av}}$ ) until observation [Rudolph and Czuba, 2000]:

$$t_{\text{av}} = \frac{1}{[\text{Oxidant}]_{\text{av}}} \frac{{}^t\delta - {}^0\delta}{{}^{12}k_{\text{ox}}\epsilon} \quad (5)$$

where  $[\text{Oxidant}]_{\text{av}}$  is the average concentration of the oxidant in the atmosphere,  ${}^0\delta$  is the isotope ratio of the emission,  ${}^t\delta$  is the isotope ratio of the analyzed compound in the field sample and  ${}^{12}k_{\text{ox}}$  is the rate constant of the oxidation reaction. Having knowledge of the isotopically determined atmospheric age of an examined compound,  $t_{\text{av}}$ , in addition to the mean concentration of the oxidant, the temporal and thus the spatial scale of the investigated process can be determined.

[9] The monoterpene  $\beta$ -pinene is one of the major biogenic VOCs emitted by forests, showing a high SOA formation potential via oxidation [Kanakidou et al., 2005] and thus, playing an important role in the aerosol-climate feedback

mechanisms within the atmosphere. In this study, the KIE of  $\beta$ -pinene ozonolysis was determined during dark chamber experiments carried out at 258 K, 273 K and 303 K. Experimental results of the temporal evolution of nopinone isotopic composition, which is the main product of  $\beta$ -pinene ozonolysis, were investigated using a modified Master Chemical Mechanism (MCM). The determined KIE values were used to calculate in the model runs the rates of the  $\beta$ -pinene ozonolysis reactions involving a  $^{13}\text{C}$  isotope.

[10] Finally, a parameterization of the observed KIE temperature dependence was deduced and 3-D global simulations of the stable carbon isotope ratio and concentration of  $\beta$ -pinene were carried out to quantify the impact of the observed KIE temperature dependence of  $\beta$ -pinene ozonolysis on global scale.

## 2. Methods

### 2.1. Experimental Method

#### 2.1.1. Experimental Conditions

[11] The  $\beta$ -pinene ozonolysis experiments were conducted at the AIDA (Aerosols Interaction and Dynamics in the Atmosphere) simulation chamber of the Karlsruhe Institute of Technology, Germany. The aerosol reactor, consisting of a cylindrical aluminum vessel of 84.5 m<sup>3</sup> volume, is housed in a dark, thermally isolated chamber and can be operated in a temperature range between 183 K and 333 K. Three working platforms around the chamber facilitate the access to reactor flanges of various sizes. Details of the AIDA chamber are described by Saathoff et al. [2003, 2009]. The three  $\beta$ -pinene ozonolysis experiments described here were performed at temperatures of 258 K, 273 K and 303 K and ambient pressure ( $\sim 1000$  hPa). Temperature and initial concentration of water and reactants are given in Table 1. The relative humidity ranged from 30 to 60%. Cyclohexane (99.5%, Merck) was used as scavenger for the OH-radicals generated during the  $\beta$ -pinene ozonolysis. Due to the high cyclohexane concentration ( $\sim 500$  ppm) used in each experiment, the examined  $\beta$ -pinene oxidation was a pure ozonolysis reaction [Saathoff et al., 2009]. Prior to each experiment, the AIDA chamber was evacuated to typically 1 Pa total pressure, flushed two times with 10 hPa of synthetic air and filled to atmospheric pressure ( $\sim 1000$  hPa) with humidified synthetic air (low hydrocarbon grade, Basi). Cyclohexane was added by flushing 9 L min<sup>-1</sup> of synthetic air over a saturator. Ozone was generated by a silent discharge generator (Semozon 030.2, Sorbios) in mixing ratios of about 3% in pure oxygen and added to the chamber either directly or after dilution in a 1 L glass bulb with a flow of 5 L min<sup>-1</sup> synthetic air. The  $\beta$ -pinene (99%, Aldrich) was evaporated up to pressures of  $\sim 2$  hPa into a 2 L glass bulb and flushed into the chamber with 10 L min<sup>-1</sup> synthetic air for 2 min. The reaction started by injecting the  $\beta$ -pinene. The stirring fan on the bottom of AIDA chamber assured an overall homogeneous mixing of all reaction components within 1–2 min. For reference purposes, upon nearly complete consumption of the reactants,  $\sim 20$  ppb nopinone (98%, Aldrich), as major product of  $\beta$ -pinene ozonolysis, was added by flushing 8 L min<sup>-1</sup> of synthetic air over a saturator containing nopinone at 50°C. In order to reach similar  $\beta$ -pinene lifetimes for all experiments, the concentrations of the reactants were varied according to Table 1.

**Table 1.** Temperature and Initial Concentration of Water, Ozone,  $\beta$ -Pinene and Nopinone for the Experiments, as well as Predicted  $\beta$ -Pinene Lifetimes Under the Given Conditions

Experiment	Temperature (K)	[H <sub>2</sub> O] (ppm)	[O <sub>3</sub> ] (ppb)	[ $\beta$ -Pinene] (ppb)	[Nopinone] (ppb)	$\tau_{\beta\text{-pinene}}$ (h)
1	303	13000	530	49	20	1.19
2	273	4500	750	44	20	1.25
3	258	1100	850	40	20	1.31

### 2.1.2. Sampling and $\delta^{13}\text{C}$ Analysis

[12] Gas phase samples were collected in pre-cleaned and evacuated Silcosteel gas canisters (Restek, Bellefonte, USA). The chamber was connected to the canisters via 6 mm PFA tubing. Ozone was removed by passing the samples through a heated Silcosteel capillary (120°C). Approximately 15 l of air were sampled by pressurizing the canisters to 2.5 bar. Blank probes for the clean chamber were taken for each experiment prior to reactant injection. Samples were collected at time intervals of 30 to 60 min. The gas phase isotopic composition was measured in the Institute for Energy and Climate Research of the Research Center Jülich within two days after samples were taken.

[13] Compound specific stable carbon isotope ratio analysis was carried out by using a setup optimized to measure gas phase samples. The system consists of a custom built cryo-sampling-thermal-desorption unit connected to a gas chromatograph coupled to an isotope ratio mass spectrometer via a combustion interface (TD-GC-IRMS).

[14] This setup was described in detail elsewhere [Iannone *et al.*, 2007; Fisseha *et al.*, 2009]. Briefly, the cryo-focusing system is custom designed (GERSTEL GmbH & Co. KG, Mülheim/Ruhr, Germany) to concentrate collected trace gases prior to separation. To this end, three successive cryo-trapping steps are used, leading to an optimal focusing of the VOCs. The first cryo-trap, a Silcosteel tube of 300 mm, 11 mm ID, packed with glass beads of 60–80 mesh, was operated at  $-170^\circ\text{C}$ . Next, the VOCs from the samples were thermally desorbed at  $240^\circ\text{C}$  and transferred with helium carrier gas to two smaller cryo-traps. The focusing was achieved through alternatively cooling-heating of these cryo-traps, from  $-170^\circ\text{C}$  to  $250^\circ\text{C}$  and from  $-80$  to  $250^\circ\text{C}$ , respectively, at a rate of  $12^\circ\text{C/s}$ . Compounds were separated with an Agilent 6890 Gas Chromatograph equipped with a Rtx-1 fused silica column (105m  $\times$  0.32mm ID, film thickness 3  $\mu\text{m}$ , Restek Corporation, Bad Homburg, Germany). For all measurements, the temperature program of the GC oven was holding  $30^\circ\text{C}$  for 5 min, ramping at a rate of  $4^\circ\text{C/min}$  to  $200^\circ\text{C}$  and holding there for 42.5 min. The separated VOCs were transferred into a combustion interface (quartz tube, packed with CuO) and oxidized at  $850^\circ\text{C}$  quantitatively to  $\text{CO}_2$  and water. The latter was removed in a cold trap at  $-100^\circ\text{C}$ , whereas the  $\text{CO}_2$  was transferred to the isotope ratio mass spectrometer (Isoprime IRMS, GV Instruments, Manchester, UK) operated in continuous flow mode for stable carbon isotope ratio measurements.

[15] The ion currents at mass-to-charge ratios  $m/z$  44, 45 and 46 were corrected for the contribution of  $^{17}\text{O}$ -containing isotopologues [Brand *et al.*, 2010].

[16] For calibration purposes, isotopic measurements of standard mixtures were performed before, in between and after the sample analyses, by using two different TD-GC-IRMS setups: the gas phase setup, described above, and an aerosol particle setup, which is optimized

for thermodesorption and transmission of the VOCs from aerosol filter samples to the GC. The systems have similar configuration, though the thermodesorption section of the latter one consists of a Thermal Desorption Unit (TDU, GERSTEL GmbH & Co. KG, Mülheim/Ruhr, Germany) mounted directly onto a Programmable Temperature Vaporizing Cooled Injection System (PTV-CIS).

[17] The standard mixtures contained n-nonane (Fluka, 99.5%), n-undecane (Merck, 99%),  $\alpha$ -pinene (Aldrich, 99%) and nopinone (Aldrich, 98%). Bulk compounds diluted in n-hexane were injected directly in the TDU of the aerosol setup. Further measurements were carried out by injecting the standard solution in glass capillary tubes filled with silane-treated fine wool, which were thermo-desorbed in the TD tube of the gas phase setup. High purity  $\text{CO}_2$  (Messer, 100%) was calibrated against IAEA standards and used as a working reference gas to calculate the  $\delta^{13}\text{C}$  of the compounds. The  $\delta^{13}\text{C}$  values of individual compounds measured using both setups are given in Table 2. Within experimental errors,  $\delta^{13}\text{C}$  values derived from both systems show good agreement.

### 2.2. Application of the Master Chemical Mechanism in the Analysis of Isotopic Measurements

[18] A gas phase near-explicit chemical scheme provided by the Master Chemical Mechanism (MCM 3.1, <http://mcm.leeds.ac.uk/MCM>) describing the degradation of VOCs in the troposphere [Jenkin *et al.*, 2003] was employed to interpret the observed time dependence of isotopic composition.

[19] Parts of the mechanism (a subset of 659 reactions with 99 compounds) were extracted by selecting  $\beta$ -pinene as primary VOC and its initial degradation products. For an explicit tracking of the  $\beta$ -pinene fraction containing  $^{13}\text{C}$  (referred to as  $^{13}\beta$ -pinene) and its oxidation products, a second set of reactions and compounds was added to get the following reaction system:

$$\left\{ \begin{array}{l} \sum_{i=1}^{659} \left( \sum_r s_r^{12} R \xrightarrow{^{12}k_i} \sum_p s_p^{12} P \right) \\ \sum_{i=1}^{659} \left( \sum_r s_r^{13} R \xrightarrow{^{12}k_i, ^{13}k_{03}} \sum_p s_p^{13} P \right) \end{array} \right. \quad (6)$$

**Table 2.**  $\delta^{13}\text{C}$  of Standards Measured Using Two TD-GC-IRMS Setups for Gas Phase and Aerosol Isotopic Analyses

Compound		Gas Phase Setup $\delta^{13}\text{C}$ (‰)	Aerosol Setup $\delta^{13}\text{C}$ (‰)
Name	Chemical Formula		
n-nonane	$\text{C}_9\text{H}_{20}$	$-43.0 \pm 0.2$	$-42.9 \pm 0.3$
n-undecane	$\text{C}_{11}\text{H}_{24}$	$-26.2 \pm 0.3$	$-26.6 \pm 0.4$
$\alpha$ -pinene	$\text{C}_{10}\text{H}_{16}$	$-27.3 \pm 0.3$	$-27.1 \pm 0.4$
nopinone	$\text{C}_9\text{H}_{14}\text{O}$	$-30.0 \pm 0.4$	$-29.7 \pm 0.5$

where  $R$  and  $P$  are reactants and products accompanied by their stoichiometric coefficients  $s_r$  and  $s_p$ , respectively.  $k_i$  represent the reaction rate coefficients of reaction  $i$ . The superscripts indicate the presence of  $^{12}\text{C}$  only or  $^{13}\text{C}$  isotope in the considered compound. Due to the low abundance of the heavier isotope, the presence of doubly or higher substituted molecules was considered negligible.  $^{13}k_{o_3}$  was solely used as the rate of  $^{13}\beta$ -pinene ozonolysis for the reactions  $^{13}\beta$ -pinene +  $\text{O}_3 \rightarrow ^{13}\text{C}_9\text{H}_{14}\text{O} + ^{13}\text{CH}_2\text{OO}$  and  $^{13}\beta$ -pinene +  $\text{O}_3 \rightarrow ^{13}\text{C}_9\text{H}_{14}\text{OO} + ^{13}\text{CH}_2\text{O}$ . Note that the superscript '13' in the products only refers to the product originating from a  $^{13}\text{C}$  containing  $\beta$ -pinene and does not specify which product carries the  $^{13}\text{C}$  atom. The rates for the rest of reactions involving  $^{13}\text{C}$  isotope were considered equal to  $^{12}k_i$ . This is legitimate since the aim of the study is to analyze the isotopic composition of  $\beta$ -pinene and nopinone during a pure ozonolysis reaction.  $^{13}k_{o_3}$  differs from  $^{12}k_{o_3}$  by the kinetic isotope effect (equation (2)). Note that within this approximate approach, possible differences of KIE for the different isotopomers are considered negligible, so the same KIE is used for all isotopomers.

[20] Additionally to the MCM reaction rates, the rate coefficient of  $^{12}\beta$ -pinene ozonolysis was employed as a function of temperature [von Hessberg et al., 2009]:

$$^{12}k_{o_3} = 1.2 \times 10^{-15} \exp^{-1300/T} \quad (7)$$

Some of the input parameters used to initialize the simulations for each experiment (temperature and initial concentration of  $\beta$ -pinene and ozone) are included in Table 1. The initial  $\delta^{13}\text{C}$  value of  $\beta$ -pinene injected into the chamber ( $-29.16\text{‰}$ ) was used to initialize the concentration of the  $^{13}\beta$ -pinene. KIE was applied as derived from the experiments (see section 3.1) to calculate the rate constant  $^{13}k_{o_3}$ .

[21] The reaction system 6, preserving the masses of the stable isotopes in the course of the reactions, was solved at each integration step. Concentrations of both  $\beta$ -pinene and nopinone isotopologues (those containing only  $^{12}\text{C}$  and those containing at least one  $^{13}\text{C}$  atom) were determined. Subsequently, the  $\delta^{13}\text{C}$  values during the ozonolysis reaction were calculated as function of reaction time.

### 2.3. Modeling Stable Carbon Isotopes With MOZART-3

[22] MOZART-3 (Model for OZone And Related Tracers, version 3) is a global chemistry transport model, described in detail by Kinnison et al. [2007]. Tropospheric chemistry mechanisms including a limited representation of non-methane hydrocarbon chemistry and monoterpene oxidation, transport, tracer advection, convection and diffusion processes as well as dry and wet deposition are simulated within the model. Vertically, 60 hybrid layers reaching from the surface to 0.1 hPa and horizontally, a grid of  $192 \times 96$  points (longitude/latitude), corresponding to a resolution of  $1.875^\circ \times 1.895^\circ$ , are used. The model time step is 15 min. 115 chemical species are involved in the simulations.  $\alpha$ - and  $\beta$ -Pinene were added to the other species, representing together the monoterpene class  $\text{C}_{10}\text{H}_{16}$ . The system of chemical reactions consists of 71 photolysis, 219 gas phase and 21 heterogeneous reactions. The gas phase reactions have been updated to JPL-06 [Sander et al., 2006].

[23] The treatment of source specific isotope fractionation in MOZART-3 is described in detail by Stein and Rudolph [2007]. The emission inventories and other input data used for the model simulations have been created for the EU FP6 project GEMS [Hollingsworth et al., 2008]. Monthly anthropogenic and natural emissions originate from the RETRO project [Schultz et al., 2007]. RETRO ship emissions have been replaced by estimates based on the work by Corbett and Koehler [2003], and East Asian anthropogenic emissions have been replaced by the REAS inventory [Ohara et al., 2007], though keeping the original RETRO seasonality. Biomass burning emissions are from the GFEDv2 inventory [van der Werf et al., 2006] giving actual wildfires with an 8-day resolution. The monoterpene emissions were split up as follows: 15% of the total monoterpenes were attributed to  $\beta$ -pinene [Spanke et al., 2001; Kanakidou et al., 2005], the rest of 85% was lumped together as  $\alpha$ -pinene emissions. The simulations for this study were driven by ECMWF ERA-Interim reanalysis [Uppala et al., 2008; Dee and Uppala, 2009] meteorology for the period March to October 2004.

[24] For our special application,  $^{12}\beta$ -pinene and  $^{13}\beta$ -pinene were introduced as separate chemical species. The temperature dependence of the rate constant of  $^{12}\beta$ -pinene ozonolysis was implemented as from equation (7). The isotopologue  $^{13}\beta$ -pinene is emitted and undergoes the same reaction pathway as  $^{12}\beta$ -pinene in the course of the simulations. The reaction rate of  $^{13}\beta$ -pinene ozonolysis was calculated from equation (2) by using the determined KIE value.

## 3. Results and Discussions

### 3.1. Tracking of Stable Isotope Composition During $\beta$ -Pinene Ozonolysis: Comparison Between Measurements and MCM Modeling

[25] The isotopic composition of  $\beta$ -pinene and nopinone (the major chromatographically separated compounds identified in the samples) was determined. The measurements of stable carbon isotope ratio and concentration of  $\beta$ -pinene were employed to calculate the ozonolysis KIE for each experiment. In turn, the experimentally obtained KIE values were employed in the initialization of MCM simulations. The progress of the isotopic composition of the major ozonolysis product, nopinone, was examined by comparing the measured values with the modeling output.

[26] Figure 1 depicts the temporal evolution of the  $\delta^{13}\text{C}$  values after the  $\beta$ -pinene injection into the AIDA reaction chamber. In all cases,  $\beta$ -pinene became enriched in the heavier isotope  $^{13}\text{C}$  during the reaction. This behavior shows that  $\beta$ -pinene ozonolysis exhibits a normal kinetic isotope effect ( $\text{KIE} > 1$ ), where the lighter isotope preferentially fractionates into the product. At 258 K, the  $\delta^{13}\text{C}$  value of  $\beta$ -pinene rises by 18.6‰ (from  $-28.9\text{‰}$  to  $-10.3\text{‰}$ ) in about 5 h after injection, compared with an increase by 15.8‰ at 273 K and 14.9‰ at 303 K respectively. For each temperature, the  $\beta$ -pinene lifetime was experimentally determined from measured concentrations. The resulting lifetimes of 1.18 h at 303 K, 1.29 h at 273 K and 1.36 h at 258 K, show good agreement with the predicted values (Table 1) with a maximum deviation of 3.7% at 258 K.

[27] In order to determine KIE, for each experiment a straight line was fitted to the experimental data according to

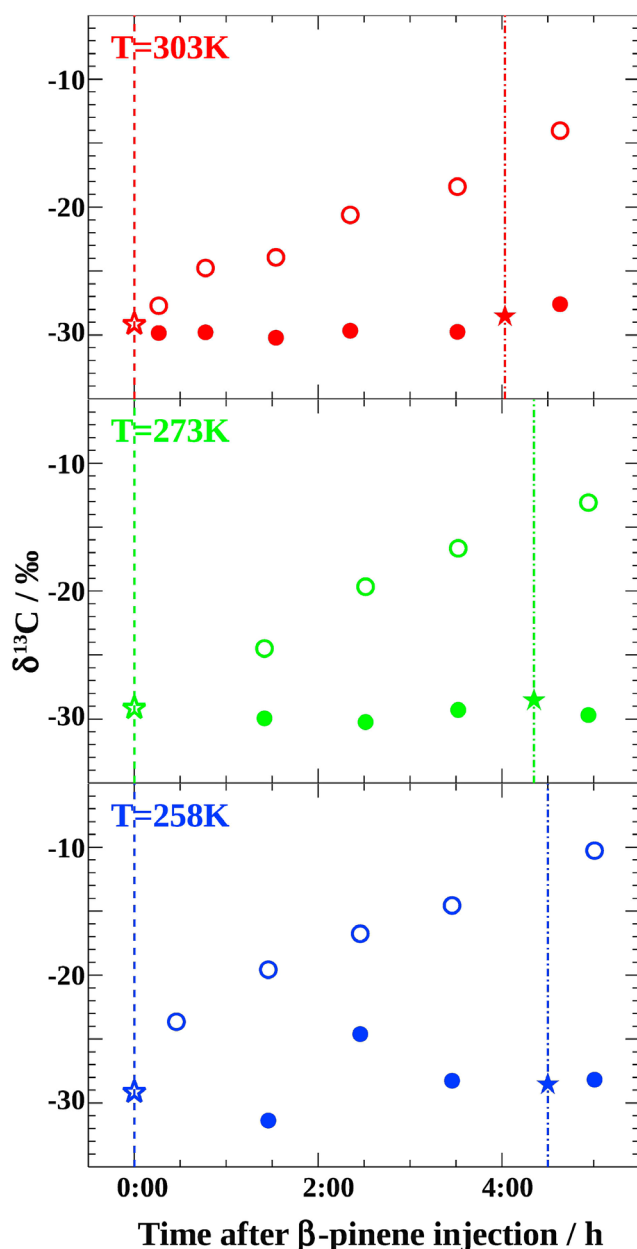


**Figure 1.** The  $\delta^{13}\text{C}$  of  $\beta$ -pinene (open circles) and gas-phase nopinone (solid circles) during the ozonolysis reaction for experiments conducted at (top) 303 K, (middle) 273 K and (bottom) 258 K. Lines indicate the time of  $\beta$ -pinene (dashed) and nopinone (dot-dashed) injection. Stars show the isotopic composition of the injected  $\beta$ -pinene (open) and nopinone (solid).

equation (4). As can be seen in Figure 2, the slope of the regression line increases with decreasing temperature. According to equation (4), the slopes of the regression lines represent  $\text{KIE}/(1 - \text{KIE})$ ; thus, KIE increases with decreasing temperature.

[28] The KIE calculated for each experiment as well as the corresponding  $\varepsilon$  values are summarized in Table 3.

[29] The average  $\varepsilon$  value for the  $\beta$ -pinene ozonolysis reaction at 303 K found in this work ( $3.58 \pm 0.13\text{‰}$ ) is higher

than the value reported by Fisseha *et al.* [2009] ( $^{\circ}\varepsilon = 2.6 \pm 1.5\text{‰}$ ), though showing agreement within the range of uncertainty. Moreover, the experimentally determined  $\varepsilon$  value at 303 K is comparable with the ozonolysis  $\varepsilon$  value of other alkenes estimated from the inverse dependence of the kinetic isotope effect on carbon number ( $N_C$ ) [Rudolph, 2007]. According to that dependence, the predicted  $^{\circ}\varepsilon$  value for  $\beta$ -pinene with  $N_C = 10$  is  $3.4 \pm 0.1\text{‰}$ . To the best of our knowledge, no literature data is available up to now on  $^{\circ}\varepsilon$  at temperatures lower than room temperature.

[30] The KIE experimental data can be well fitted by a mono-exponential-plus-constant function dependent on temperature (Figure 3):

$$\text{KIE} = 1.0035038 + 6.85 \times 10^{-14} \exp^{6198.84/T} \quad (8)$$

For the achieved measurement precision of 0.13‰ (see Table 3), the results obtained by using the regression equation (8) indicate that a change in KIE with temperature is experimentally not distinguishable at temperatures higher than 284 K. This conclusion is consistent with the work of Anderson [2005], who showed that for a series of VOC oxidation experiments carried out at temperatures higher than 288 K, no significant KIE temperature dependence could be established within their measurement precision. Note that applying equation (8) outside the temperature range within which experiments were performed may result in uncertainties, specifically for temperatures lower than 258 K.

[31] The  $\delta^{13}\text{C}$  values of gas-phase nopinone vary between  $-30.3\text{‰}$  and  $-25.1\text{‰}$  (Figure 1). Similar to the  $\beta$ -pinene, gas-phase nopinone became overall heavier during the ozonolysis reaction, but the increase of nopinone  $\delta^{13}\text{C}$  values in the course of the experiments was only very slight. The isotopic composition of the first generation oxidation product nopinone depends on factors involved in both, its chemical formation and removal processes, together with their associated KIEs. First, assuming that KIE in  $\beta$ -pinene ozonolysis reaction forming nopinone primarily determines the nopi-

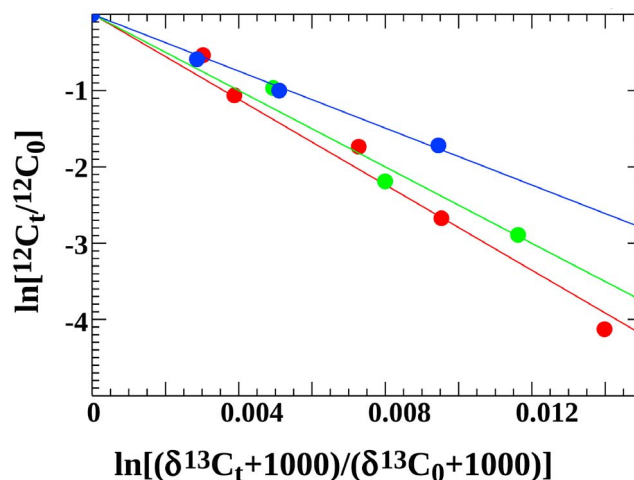


**Figure 2.** Linear regression of experimental data to determine KIE values of  $\beta$ -pinene ozonolysis at 303 K (red), 273 K (green) and 258 K (blue).

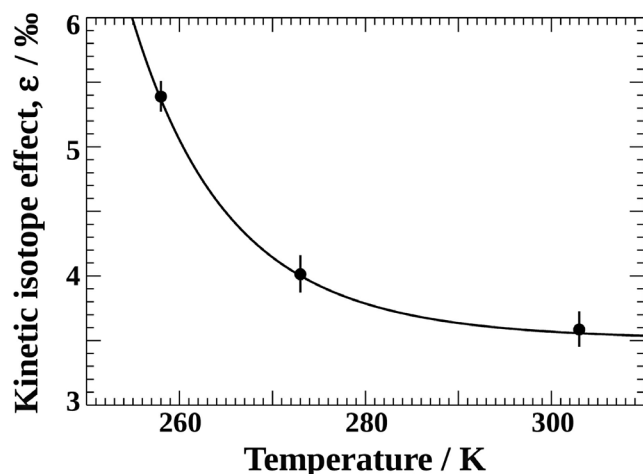
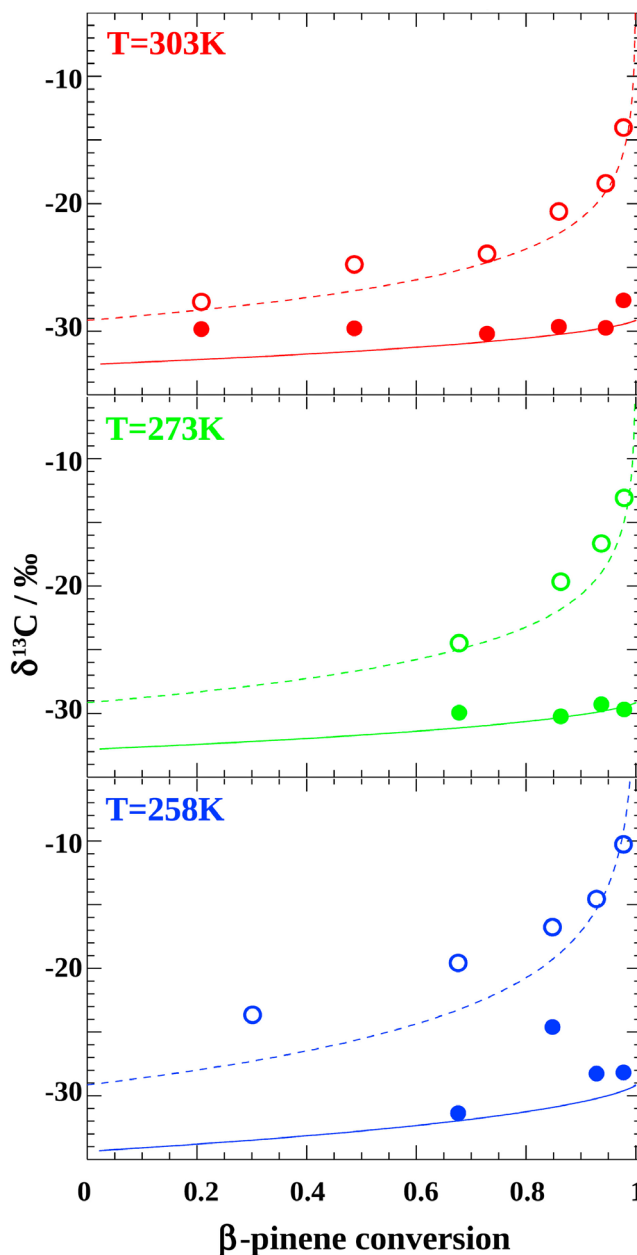
**Table 3.** KIE and  $\epsilon$  Values of  $\beta$ -Pinene Ozonolysis at Different Temperatures

Temperature (K)	Data Points	Slope = $\frac{\text{KIE}}{1 - \text{KIE}}$	R <sup>2</sup>	KIE	$\text{O}_3\epsilon$ (‰)
303	6	-279.59	0.98	$1.00358 \pm 0.00013$	$3.58 \pm 0.13$
273	4	-250.20	0.96	$1.00380 \pm 0.00014$	$3.80 \pm 0.14$
258	4	-186.56	0.99	$1.00539 \pm 0.00012$	$5.39 \pm 0.12$

none  $\delta^{13}\text{C}$  composition, a nopinone  $\delta^{13}\text{C}$  value lower than the precursor  $\delta^{13}\text{C}$  value by the KIE is expected at early stages. Additionally, after full oxidation of all  $\beta$ -pinene existing in the system, nopinone  $\delta^{13}\text{C}$  value should be equal to the initial  $\delta^{13}\text{C}$  value of  $\beta$ -pinene. Second, chemical and condensational loss processes should influence the evolution of nopinone isotopic composition. Since OH radicals were efficiently scavenged during the experiments, chemical loss of nopinone can be excluded from the factors controlling its isotopic composition. Finally, condensational processes during oxidation reactions should not significantly affect  $\delta^{13}\text{C}$  evolution. Fisseha *et al.* [2009] report an average fractionation of 2.3‰ for the partitioning of nopinone in the aerosol in an experiment using no OH scavenger. Irei *et al.* [2006, 2011] show that for toluene oxidation, only the first reaction step determines the isotopic composition, thus fractionation due to partitioning into particulate matter can be neglected.

[32] To explore the controlling factors of the measured temporal evolution of nopinone isotopic composition, the hypothesis is tested that the nopinone formation from  $\beta$ -pinene ozonolysis with its determined KIE is dominating the  $\delta^{13}\text{C}$  evolution of nopinone. To this end, MCM simulations were carried out, as described in section 2.2. The runs were initialized with the experimentally obtained KIE values (Table 3). Figure 4 shows measured and modeled  $\delta^{13}\text{C}$  values of  $\beta$ -pinene and nopinone as function of the fractional conversion of  $\beta$ -pinene.

[33] The MCM curves show that, as the reaction progresses,  $\delta^{13}\text{C}$  of  $\beta$ -pinene increases. The  $\delta^{13}\text{C}$  of the nopinone produced from the  $\beta$ -pinene ozonolysis rises too. The difference between the initial and final  $\delta^{13}\text{C}$  values of nopinone is yet smaller than for the  $\beta$ -pinene. At the beginning of the

**Figure 3.** Exponential regression of experimental data to determine the KIE temperature dependence.**Figure 4.** Comparison between experimental data and modeled  $\delta^{13}\text{C}$  of  $\beta$ -pinene and gas-phase nopinone during the ozonolysis reaction as function of fractional  $\beta$ -pinene conversion. The lines indicate the simulation results for the  $\beta$ -pinene (dashed) and nopinone (solid) isotopic composition in the course of reaction. The circles represent  $\delta^{13}\text{C}$  experimental data of  $\beta$ -pinene (open) and nopinone (solid).



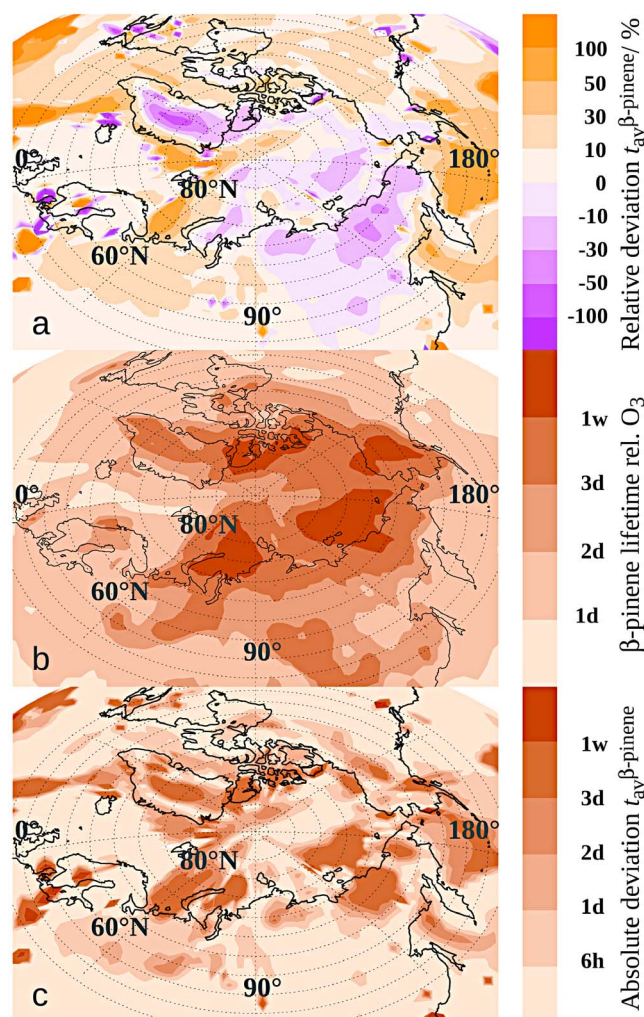


**Figure 5.** Modeled (a) relative and (c) absolute difference in the isotopically determined atmospheric age of  $\beta$ -pinene near the surface on 1 April 2004 between scenarios ‘\_T’ (including KIE temperature dependence of  $\beta$ -pinene oxidation) and ‘\_0’ (neglecting the KIE temperature dependence). (b) Also shown is the modeled  $\beta$ -pinene lifetime with respect to the reaction with ozone near the surface on 1 April 2004. For Figures 5b and 5c: h = hours, d = days, w = weeks.

reaction, the modeled  $\delta^{13}\text{C}$  values of  $\beta$ -pinene and nopinone differ by the exact amount dictated by the KIE. Since the reaction is assumed to be a closed system, where only one product forms and is not removed, the  $\delta^{13}\text{C}$  value of the nopinone at the end of the reaction is equal to the initial  $\delta^{13}\text{C}$  value of  $\beta$ -pinene [Schmidt *et al.*, 2004]. Note that the assumption of no effective nopinone loss occurring in the course of the experiments will affect nopinone gas-phase concentrations and, by that, the  $\delta^{13}\text{C}$  of the modeled nopinone. The semivolatile nopinone is known to partition into the secondary organic aerosol formed during  $\beta$ -pinene ozonolysis [Pathak *et al.*, 2008; Hohaus *et al.*, 2010], yet associated with a small isotope fractionation (see above). Therefore, for the  $\delta^{13}\text{C}$  modeling, nopinone partitioning between gas and particle phase was neglected.

[34] Within the error range, good agreement between measured and predicted  $\delta^{13}\text{C}$  values of nopinone was found at high degree of  $\beta$ -pinene processing. Discrepancies between modeled and measured nopinone  $\delta^{13}\text{C}$  exist for early stages of the reaction (see Figure 4). Overall, the observed isotopic composition of nopinone is mainly driven by the chemical processes involved in its formation and the associated KIE. For high degrees of  $\beta$ -pinene processing nopinone loss processes can be neglected.

### 3.2. Temperature Dependence of KIE and Its Application in Ambient Atmospheric Studies of VOCs

[35] In order to test the effect of an increasing KIE at lower temperature on global isotope distribution and the inferred photochemical age, the temperature dependence of KIE was implemented in 3-D simulations of the stable carbon isotope ratio and concentration of  $\beta$ -pinene. A sensitivity study was carried out with the global chemistry transport model MOZART (Model for Ozone And Related Tracers, version 3):

[36] 1. Under the base case scenario (‘\_0’), no temperature dependence of KIE was considered;

[37] 2. Under the temperature dependency scenario (‘\_T’) the temperature dependence of KIE (equation (8)) was implemented in the calculations.

[38] For case ‘\_T’,  $^{13}k_T$  was calculated at each model step, taking into account the temperature dependence of KIE (equations (2), (7) and (8)). For case ‘\_0’, a parallel simulation was carried out, neglecting the temperature dependence of  $\beta$ -pinene ozonolysis KIE.

[39] Among all simulations, the near surface results from 1 April 2004, 15:00 UT are presented. Special emphasis is put on the boreal needleleaf forests, which cover a broad swath of land, typically north of  $50^\circ$  north latitude to beyond the Arctic Circle (after the International Global Biosphere Programme IGBP classification [Friedl *et al.*, 2002]). Boreal biogenic VOC emissions are dominated by monoterpenes and among them,  $\beta$ -pinene emissions are significant [Tarvainen *et al.*, 2005, and references therein]. Note that maximum differences between the two model runs are expected when choosing early spring for the analyses. At that time of the year, low temperatures still prevail in the boreal zone, thus intensifying the divergence in the  $\beta$ -pinene isotopic composition calculated using the test versus the base case. The temperature on 1 April 2004 varies between 250 K and 280 K, with median value of 265 K. Furthermore, high monoterpene emissions are reached soon after bud burst in March/April [Hakola *et al.*, 2001].

[40] As indicated in section 1, average atmospheric age  $t_{av}$  can be derived basing on known source isotopic composition and KIE. As a consequence, the differences in  $\beta$ -pinene isotopic composition generated by taking into account the temperature dependence of KIE, compared with the ‘\_0’ base case, will result in a modified calculated  $t_{av}$ . The model output data sets from the sensitivity runs ‘\_T’ and ‘\_0’ are depicted in Figure 5a in form of

$$\Delta_{rel}t_{av} = \left( \frac{t_{av-T}}{t_{av-0}} - 1 \right) 100$$

This relative value describes how much a determined  $t_{av}$  can differ from its real value when ignoring the KIE

**Table 4.** Sign and Magnitude of  $t_{av}$  Deviations Depending on Temperature and Age of the Observed Air Masses<sup>a</sup>

Case	Temperature	Age	$X_\varepsilon = \frac{\varepsilon_-0}{\varepsilon_-T}$	$X_\delta = \frac{t_{\delta-T} - t_{\delta-0}}{t_{\delta-0} - t_{\delta}}$	$\frac{t_{av-T}}{t_{av-0}} - 1$
1	low <sup>b</sup>	fresh air masses	$\ll 1$	$\approx 1$	negative
2	low <sup>b</sup>	old air masses	$\ll 1$	$\gg 1$	negative/positive
3	high <sup>c</sup>	old air masses	$\approx 1$	$\geq 1$	positive

<sup>a</sup>See text for a detailed discussion of the temperature dependence of  $X_\delta$  and  $X_\varepsilon$ .

<sup>b</sup>Below 280 K.

<sup>c</sup>Higher than 280 K.

temperature dependence in the atmospheric calculations and can be expressed by using equation (5) as follows:

$$\Delta_{rel}t_{av} = \left( \frac{t_{\delta-T} - t_{\delta-0}}{X_\delta} \frac{\varepsilon_-0}{X_\varepsilon} - 1 \right) 100 \quad (9)$$

The variation with the temperature of the terms  $X_\delta$ , referring to the isotopic fractionation of the examined compound from emission to observation, and  $X_\varepsilon$ , involving the KIE of the chemical degradation, will determine the sign and magnitude of  $\Delta_{rel}t_{av}$ , as discussed in further detail below. The extent of  $X_\delta$  is controlled by two factors, temperature and age of observed air masses. Near the source, the fractionation is small at any temperature, thus  $X_\delta \approx 1$ . Temperature dependence of  $X_\delta$  becomes important for old air masses, in which the  $^{13}\text{C}$  enrichment of reactants is higher at low temperature (Figure 4). The lower the temperature, the higher  $t_{\delta-T} - t_{\delta-0}$  in comparison with  $t_{\delta-0} - t_{\delta}$ . According to this,  $X_\delta$  in old air masses is equal to unity at room temperature and higher than 1 at lower temperature. Other than  $X_\delta$ ,  $X_\varepsilon$  is always lower or equal to unity and depends on temperature alone. At room temperature,  $\varepsilon_-T$  is similar to  $\varepsilon_-0$ , therefore  $X_\varepsilon \approx 1$ . At lower temperature,  $\varepsilon_-T$  is higher than  $\varepsilon_-0$  (Figure 3); hence  $X_\varepsilon$  is lower than 1. All these temperature-dependent changes of  $X_\delta$  and  $X_\varepsilon$  as well as the resulting overall relative change in atmospheric age  $\Delta_{rel}t_{av}$  are summarized in Table 4. Summing up, at low temperature and for fresh air masses (i.e., close to the source)  $\Delta_{rel}t_{av}$  is negative. At low temperature but in older air masses, the  $t_{av}$  deviation can be either negative or positive, depending on the concurrence between  $X_\varepsilon$  and  $X_\delta$ . Finally,  $\Delta_{rel}t_{av}$  is positive in old air masses at higher temperature.

[41] As can be seen in Figure 5a, negative values of  $\Delta_{rel}t_{av}$  in the Asian boreal zone suggest strong fresh monoterpene emissions at lower temperature (case 1 in Table 4), contrasting to the European part, where the  $X_\delta$  term becomes dominant because of the older air masses, thus leading to slightly positive  $\Delta_{rel}t_{av}$ . This observation might be explained by the unlike structure of the vegetation. The western part of the boreal zone is dominated by ‘evergreen needleleaf forests (IGBP 1),’ while the eastern part is covered by ‘deciduous needleleaf forests (IGBP 3),’ the latter showing higher monoterpene emission potential in the budding season. These areas are continuously supplied with significant freshly emitted monoterpenes, therefore negative  $\Delta_{rel}t_{av}$  values predominate. Very old air masses, character-

ized by strong  $X_\delta$  term can be detected over the oceans. Examining the magnitude of  $\Delta_{rel}t_{av}$ , relative deviations in determined  $\beta$ -pinene  $t_{av}$  of up to 30% in the Asian and North American boreal zone can arise. There are also smaller areas in central Sweden, Eastern Finland and Eastern Canada, where the calculated  $t_{av}$  might be even two times over- (case 1 in Table 4) or underestimated (case 3 in Table 4). Neglecting the temperature dependence of KIE in evaluations of the average atmospheric age of a species may therefore play an important role in the interpretation of the VOCs atmospheric processing. The simulations also indicate very low concentrations of OH radicals prevailing in the boreal early spring. Therefore, the atmospheric residence time of  $\beta$ -pinene is more strongly controlled by its reaction with ozone. Taking this into account, median  $\beta$ -pinene lifetime of 52.7 h in the boreal forests are computed (Figure 5b). Note that for room temperature and typical atmospheric  $\text{O}_3$  concentration levels,  $\beta$ -pinene lifetime is about 1.1 days [Atkinson and Arey, 2003]. Given the aforementioned considerations, neglecting the temperature dependence of KIE, the absolute  $\beta$ -pinene average age  $t_{av}$ , isotopically determined, is over- or underestimated by up to one day in the calculations (Figure 5c).

#### 4. Summary

[42] This study reports for the first time  $\text{O}_3\varepsilon$  values for temperatures lower than room temperature. The  $\text{O}_3\varepsilon$  values of  $\beta$ -pinene ozonolysis at 273 K and 258 K are  $3.80 \pm 0.14\text{‰}$  and  $5.39 \pm 0.12\text{‰}$ , respectively. At 303 K, the  $\text{O}_3\varepsilon$  value of  $3.58 \pm 0.13\text{‰}$  shows agreement with results of Fisseha et al. [2009]. It supports also the inverse KIE dependence on the carbon number [Rudolph, 2007] being an apt method to estimate the KIE of VOC oxidation reactions.

[43] According to these findings, KIE increases with decreasing temperature. The KIE temperature dependence of  $\beta$ -pinene ozonolysis can be described as follows:

$$\text{KIE} = 1.0035038 + 6.85 \times 10^{-14} \exp^{6198.84/T}$$

Considering measurement error, the KIE temperature dependence becomes significant at temperatures lower than 284 K. Such temperatures are commonly found in the boreal needleleaf forests, which are a major source of  $\beta$ -pinene. The KIE temperature dependence was hence implemented in global modeling calculations of  $\beta$ -pinene stable carbon isotope ratio and concentration, with emphasis on boreal zones. The simulations carried out with the global chemistry transport model MOZART-3 show that ignoring the temperature dependence of KIE in the calculations might lead to noticeable over- or underestimation of the  $\beta$ -pinene atmospheric average age in the investigated regions. The consequence might be an inaccurate interpretation of the spatial scale of studied processes. Since the BVOC emissions are constrained by low temperature, we expect severe effects from KIE temperature dependence in case of VOCs with emissions independent of temperature. Future experiments should explore the effect of temperature on KIE in oxidation reactions of anthropogenic and biogenic VOCs, covering the full range of temperatures relevant for the troposphere.

[44] Furthermore the use of a simplified MCM to predict  $\delta^{13}\text{C}$  values of the major  $\beta$ -pinene oxidation product,



nopinone, shows that the tested hypothesis that the chemical formation of nopinone and the related KIE are the determining factors in the evolution of its isotopic composition can be applied at high degrees of  $\beta$ -pinene processing. Early stages of the reaction may involve nopinone loss processes that affect its isotopic composition and this should be explored in future experiments.

[45] **Acknowledgments.** We thank Jochen Rudolph (York University, Toronto) for fruitful discussions and valuable suggestions. We also gratefully acknowledge the AIDA scientific team for constant advice and assistance during the measurement campaign. This work was supported by the EU within the EUROCHAMP project. We thank Angelika Heil for providing us with IGBP Moderate resolution Imaging Spectroradiometer (MODIS) Land Cover data.

## References

- Anderson, R. S. (2005), Carbon kinetic isotope effects in the gas-phase reactions of non-methane hydrocarbons with hydroxyl radicals and chlorine atoms, Ph.D. dissertation, York Univ., Toronto, Ont., Canada.
- Anderson, R. S., E. Czuba, D. Ernst, L. Huang, A. E. Thompson, and J. Rudolph (2003), Method for measuring carbon kinetic isotope effects of gas-phase reactions of light hydrocarbons with the hydroxyl radical, *J. Phys. Chem. A*, **107**, 6191–6199, doi:10.1021/jp034256d.
- Anderson, R. S., L. Huang, R. Iannone, and J. Rudolph (2004a), Carbon kinetic isotope effects in the gas phase reactions of light alkanes and ethene with the OH radical at  $296 \pm 4$  K, *J. Phys. Chem. A*, **108**(52), 11537–11544, doi:10.1021/jp0472008.
- Anderson, R. S., R. Iannone, A. E. Thompson, J. Rudolph, and L. Huang (2004b), Carbon kinetic isotope effects in the gas-phase reactions of aromatic hydrocarbons with the OH radical at  $296 \pm 4$  K, *Geophys. Res. Lett.*, **31**, L15108, doi:10.1029/2004GL020089.
- Atkinson, R., and J. Arey (2003), Gas-phase tropospheric chemistry of biogenic volatile organic compounds: A review, *Chem. Rev.*, **103**, 4605–4638, doi:10.1021/cr0206420.
- Brand, W. A., S. S. Assonov, and T. B. Coplen (2010), Correction for the  $^{17}\text{O}$  interference in  $\delta(^{13}\text{C})$  measurements when analyzing  $\text{CO}_2$  with stable isotope mass spectrometry (IUPAC Technical Report), *Pure Appl. Chem.*, **82**(8), 1719–1733, doi:10.1351/PAC-REP-09-01-05.
- Corbett, J. J., and H. W. Koehler (2003), Updated emissions from ocean shipping, *J. Geophys. Res.*, **108**(D20), 4650, doi:10.1029/2003JD003751.
- Dee, D., and S. M. Uppala (2009), Variational bias correction of satellite radiance data in the ERA–Interim reanalysis, *Q. J. R. Meteorol. Soc.*, **135**, 1830–1841, doi:10.1002/qj.493.
- Fisseha, R., H. Spahn, R. Wegener, T. Hohaus, G. Brasse, H. Wissel, R. Tillmann, A. Wahner, R. Koppmann, and A. Kiendler-Scharr (2009), Stable carbon isotope composition of secondary organic aerosol from  $\beta$ -pinene oxidation, *J. Geophys. Res.*, **114**, D02304, doi:10.1029/2008JD011326.
- Friedl, M. A., D. K. McIver, J. C. F. Hodges, X. Y. Zhang, D. Muchoney, A. H. Strahler, C. E. Woodcock, S. Gopal, A. Schneider, and A. Cooper (2002), Global land cover mapping from MODIS: Algorithms and early results, *Remote Sens. Environ.*, **83**, 287–302, doi:10.1016/S0034-4257(02)00078-0.
- Guenther, A. (1999), Modeling biogenic volatile organic compound emissions to the atmosphere, in *Reactive Hydrocarbons in the Atmosphere*, edited by C. N. Hewitt, pp. 97–118, Academic, San Diego, Calif., doi:10.1016/B978-012346240-4/50004-7.
- Guenther, A., et al. (1995), Global model of natural volatile organic-compound emissions, *J. Geophys. Res.*, **100**(D5), 8873–8892, doi:10.1029/94JD02950.
- Hakola, H., T. Laurila, V. Lindfors, H. Hellen, A. Gaman, and J. Rinne (2001), Variation of the VOC emission rates of birch species during the growing season, *Boreal Environ. Res.*, **6**(3), 237–249.
- Hohaus, T., et al. (2010), A new aerosol collector for quasi on-line analysis of particulate organic matter: The Aerosol Collection Module (ACM) and first applications with a GC/MS-FID, *Atmos. Meas. Tech.*, **3**(5), 1423–1436, doi:10.5194/amt-3-1423-2010.
- Hollingsworth, A., et al. (2008), Toward a monitoring and forecasting system for atmospheric composition: The GEMS project, *Bull. Am. Meteor. Soc.*, **89**, 1147–1164, doi:10.1175/2008BAMS2355.1.
- Iannone, R., R. S. Anderson, J. Rudolph, L. Huang, and D. Ernst (2003), The carbon kinetic isotope effects of ozone-alkene reactions in the gas-phase and the impact of ozone reactions on the stable carbon isotope ratios of alkenes in the atmosphere, *Geophys. Res. Lett.*, **30**(13), 1684, doi:10.1029/2003GL017221.
- Iannone, R., R. Koppmann, and J. Rudolph (2007), A technique for atmospheric measurements of stable carbon isotope ratios of isoprene, methacrolein, and methyl vinyl ketone, *J. Atmos. Chem.*, **58**, 181–202, doi:10.1007/s10874-007-9087-5.
- International Union of Pure and Applied Chemistry, Commission on Atomic Weights and Isotopic Abundances (IUPAC) (1994), Atomic weights of the elements 1993, *Pure Appl. Chem.*, **66**, 2423–2444, doi:10.1351/pac199466122423.
- Irei, S., L. Huang, F. Collina, W. Zhang, D. Hastie, and J. Rudolph (2006), Flow reactor studies of the stable carbon isotope composition of secondary particulate organic matter generated by OH-radical-induced reactions of toluene, *Atmos. Environ.*, **40**, 5858–5867, doi:10.1016/j.atmosenv.2006.05.001.
- Irei, S., J. Rudolph, L. Huang, J. Auld, and D. Hastie (2011), Stable carbon isotope ratio of secondary particulate organic matter formed by photooxidation of toluene in indoor smog chamber, *Atmos. Environ.*, **45**, 856–862, doi:10.1016/j.atmosenv.2010.11.021.
- Jenkin, M. E., S. M. Saunders, V. Wagner, and M. J. Pilling (2003), Protocol for the development of the Master Chemical Mechanism, MCM v3(Part B): Tropospheric degradation of aromatic volatile organic compounds, *Atmos. Chem. Phys.*, **3**, 181–193, doi:10.5194/acp-3-181-2003.
- Kanakidou, M., et al. (2005), Organic aerosol and global climate modelling: A review, *Atmos. Chem. Phys.*, **5**, 1053–1123, doi:10.5194/acp-5-1053-2005.
- Kinnison, D. E., et al. (2007), Sensitivity of chemical tracers to meteorological parameters in the MOZART-3 chemical transport model, *J. Geophys. Res.*, **112**, D20302, doi:10.1029/2006JD007879.
- Müller, J.-F. (1992), Geographical distribution and seasonal variation of surface emissions and deposition velocities of atmospheric trace gases, *J. Geophys. Res.*, **97**(D4), 3787–3804, doi:10.1029/91JD02757.
- Ohara, T., H. Akimoto, J. Kurokawa, N. Horii, K. Yamaji, X. Yan, and T. Hayasaka (2007), An Asian emission inventory of anthropogenic emission sources for the period 1980–2020, *Atmos. Chem. Phys.*, **7**, 4419–4444, doi:10.5194/acp-7-4419-2007.
- Pathak, R., N. M. Donahue, and S. N. Pandis (2008), Ozonolysis of  $\beta$ -pinene: Temperature dependence of secondary organic aerosol mass fraction, *Environ. Sci. Technol.*, **42**(14), 5081–5086, doi:10.1021/es070721z.
- Piccot, S. D., J. J. Watson, and J. W. Jones (1992), A global inventory of volatile organic compound emissions from anthropogenic sources, *J. Geophys. Res.*, **97**(D9), 9897–9912, doi:10.1029/92JD00682.
- Rudolph, J. (2007), Gas chromatography–isotope ratio mass spectrometry, in *Volatile Organic Compounds in the Atmosphere*, edited by R. Koppmann, pp. 388–466, Blackwell, Oxford, U. K., doi:10.1002/9780470988657.ch10.
- Rudolph, J., and E. Czuba (2000), On the use of isotopic composition measurements of volatile organic compounds to determine the “photochemical age” of an air mass, *Geophys. Res. Lett.*, **27**(23), 3865–3868, doi:10.1029/2000GL011385.
- Saathoff, H., O. Mohler, U. Schurath, S. Kamm, B. Dippel, and D. Mihelcic (2003), The AIDA soot aerosol characterisation campaign 1999, *J. Aerosol Sci.*, **34**, 1277–1296, doi:10.1016/S0021-8502(03)00363-X.
- Saathoff, H., K. H. Naumann, O. Mohler, A. M. Jonsson, M. Hallquist, A. Kiendler-Scharr, T. F. Mentel, R. Tillmann, and U. Schurath (2009), Temperature dependence of yields of secondary organic aerosols from the ozonolysis of alpha-pinene and limonene, *Atmos. Chem. Phys.*, **9**(5), 1551–1577, doi:10.5194/acp-9-1551-2009.
- Sander, S. P., et al. (2006), Chemical kinetics and photochemical data for use in atmospheric studies, *Evaluation 15*, *JPL Publ.*, **06-2**, 15 pp.
- Schmidt, T. C., L. Zwank, M. Elsner, M. Berg, R. U. Meckenstock, and S. B. Haderlein (2004), Compound-specific stable isotope analysis of organic contaminants in natural environments: A critical review of the state of the art, prospects, and future challenges, *Anal. Bioanal. Chem.*, **378**(2), 283–300, doi:10.1007/s00216-003-2350-y.
- Schultz, M. G., et al. (2007), REanalysis of the TROpospheric chemical composition over the past 40 years: A long-term global modeling study of tropospheric chemistry funded under the 5th EU framework programme, *Rep. Earth Syst. Sci.*, **48/2007**, Max Planck Inst., Hamburg, Germany.
- Spanke, J., U. Rannik, R. Forkel, W. Nigge, and T. Hoffmann (2001), Emission fluxes and atmospheric degradation of monoterpenes above a boreal forest: Field measurements and modelling, *Tellus, Ser. B*, **53**, 406–422, doi:10.1034/j.1600-0889.2001.d01-29.x.
- Stein, O., and J. Rudolph (2007), Modeling and interpretation of stable carbon isotope ratios of ethane in global chemical transport models, *J. Geophys. Res.*, **112**, D14308, doi:10.1029/2006JD008062.
- Tarvainen, V., H. Hakola, H. Hellen, J. Back, P. Hari, and M. Kulmala (2005), Temperature and light dependence of the VOC emissions of

- Scots pine, *Atmos. Chem. Phys.*, 5, 989–998, doi:10.5194/acp-5-989-2005.
- Uppala, S. M., D. Dee, S. Kobayashi, P. Berrisford, and A. Simmons (2008), Towards a climate data-assimilation system: Status update of ERA–Interim, *ECMWF Newsl.*, 115, 12–18.
- van der Werf, G. R., J. T. Randerson, L. Giglio, G. J. Collatz, P. S. Kasibhatla, and A. F. Arellano Jr. (2006), Interannual variability in global biomass burning emissions from 1997 to 2004, *Atmos. Chem. Phys.*, 6, 3423–3441, doi:10.5194/acp-6-3423-2006.
- von Hessberg, C., P. von Hessberg, U. Poschl, M. Bilde, O. J. Nielsen, and G. K. Moortgat (2009), Temperature and humidity dependence of secondary organic aerosol yield from the ozonolysis of  $\beta$ -pinene, *Atmos. Chem. Phys.*, 9, 3583–3599, doi:10.5194/acp-9-3583-2009.
- Wang, H., and K. Kawamura (2006), Stable carbon isotopic composition of low-molecular-weight dicarboxylic acids and ketoacids in remote marine aerosols, *J. Geophys. Res.*, 111, D07304, doi:10.1029/2005JD006466.
- 
- I. Gensch, B. Kammer, A. Kiendler-Scharr, W. Laumer, O. Stein, A. Wahner, and R. Wegener, Institut für Energie- und Klimaforschung, Troposphäre (IEK-8), Forschungszentrum Jülich GmbH, Wilhelm-Johnen-Str., D-52425 Jülich, Germany. (a.kiendler-scharr@fz-juelich.de)
- T. Hohaus, Aerodyne Research, Inc., 45 Manning Rd., Billerica, MA 01821-3976, USA.
- H. Saathoff, Institute for Meteorology and Climate Research (IMK-AAF), Karlsruhe Institute of Technology, D-76344 Karlsruhe, Germany.